

Microstructured optical fiber for single-polarization air guidance

A. Argyros and N. Issa

*Australian Photonics Cooperative Research Centre, Optical Fibre Technology Centre and School of Physics,
University of Sydney, Sydney, NSW 2006, Australia*

I. Bassett and M. A. van Eijkelenborg

*Australian Photonics Cooperative Research Centre, Optical Fibre Technology Centre,
University of Sydney, Sydney, NSW 2006, Australia*

Received June 18, 2003

An air-core microstructured fiber design that supports a single-polarization, circularly symmetric nondegenerate mode is presented. The fiber design is modeled directly, and the microstructured cladding is analyzed by use of band diagrams to elucidate the mechanism through which polarization nondegeneracy is achieved.

© 2004 Optical Society of America

OCIS codes: 060.2280, 060.2430, 230.3990, 260.5430.

Microstructured optical fibers and photonic bandgap (PBG) fibers have received much attention in recent years.¹ They offer the ability to attain properties that are unattainable in conventional fibers, such as single-mode operation over a large wavelength range² and guidance in an air core.³ Here a design is presented for a microstructured fiber that isolates a single-polarization circularly symmetric mode.

Most single-mode optical fibers support two degenerate, orthogonally polarized modes. Perturbations in the fiber's structure and external forces on the fiber can create asymmetries that break the polarization degeneracy, resulting in polarization mode dispersion and polarization fading in interferometers. Stress-induced or geometrical birefringence can be used to overcome these problems by minimizing coupling between the two polarization modes or by eliminating one polarization altogether.^{4,5} These approaches can produce a single-polarization nondegenerate mode fiber, but all isolate a linear polarization, meaning that orientation issues arise with respect to coupling, splicing, and some sensing applications.

Recently, an air-core PBG fiber design was shown to isolate a single polarization mode while it retained circular symmetry.⁶ This Bragg fiber supported only a TE mode, rather than a linearly polarized mode. The TE mode was isolated by superimposing the Bragg and Brewster angle conditions, producing a single-polarization bandgap (at the Brewster angle, TM-polarized light is not reflected). The TE-only bandgap eliminates the need for birefringence, allowing the design to be circularly symmetric. In this Letter we show that the same modal properties are possible in a microstructured PBG fiber by modeling the fiber directly and by analyzing the band diagrams of the microstructured cladding.

The design is an air-core ring-structured fiber⁷ (Fig. 1). The rings of holes are described by two pitch or hole spacing parameters, Λ_i for the intraring pitch and Λ_e for the interring pitch, and hole diameter

d . The design presented here has $\Lambda_i = 0.403 \mu\text{m}$, $\Lambda_e = 0.578 \mu\text{m}$, $d = 0.335 \mu\text{m}$, and core radius $r_{co} = 2.89 \mu\text{m}$, giving $d/\Lambda_i = 0.83$. The host material was assumed to be lossless, with a refractive index of 1.49 [corresponding to poly(methyl methacrylate) material], and the number of rings of holes was varied.

Previous research with ring-structured fibers⁷ showed that each ring of holes behaves as a discrete homogeneous ring of low refractive index. It is clear that such homogenization applied to the design in Fig. 1 produces the refractive-index profile of a Bragg fiber. It is this result that inspired the design presented here, and the values of the various parameters were chosen such that the azimuthal arithmetic mean of the index profile emulates that of the TE Bragg fiber reported earlier.⁶

We modeled the design to determine the confinement loss as a function of wavelength and the number of rings of holes. The results for the leaky modes with the lowest confinement loss are presented in Fig. 2. The adjustable boundary condition method⁸ that is capable of calculating confinement loss, with finite-difference discretization in the radial direction and Fourier decomposition in the azimuthal direction, was used in the modeling. Although the design here is not strictly circularly symmetric, it has a high rotational symmetry (ninefold), and the modes that

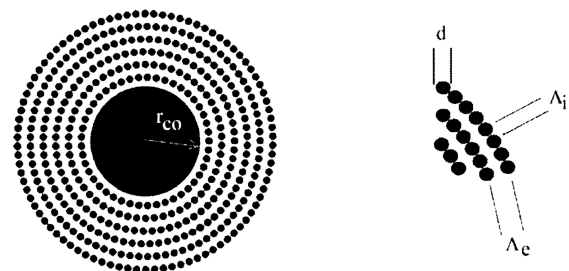


Fig. 1. Cross section of a microstructured PBG fiber design with six rings.

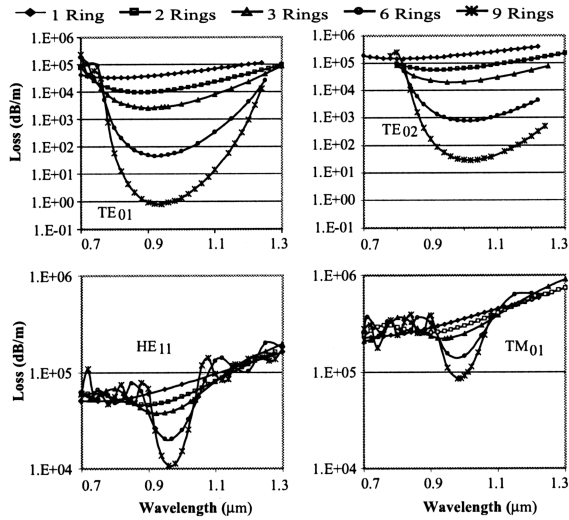


Fig. 2. Confinement loss as a function of wavelength and of the number of rings for TE_{01} , TE_{02} , HE_{11} , and TM_{01} modes. The loss of the TE_{01} mode exhibits the largest decrease as rings are added, indicating the development of a TE bandgap centered near 940 nm.

are supported closely resemble the modes of circularly symmetric waveguides. For this reason the modes are labeled in the same way as in standard fibers and are thus TE-, TM-, and HE-like. The ninefold symmetry was forced on the structure to speed up calculations and is not required in the design for any other reason.

Figure 2 shows the confinement loss of the TE modes decreasing significantly as the number of rings of holes increases, whereas this does not occur for the TM- and HE-polarized modes. Going from one to nine rings decreases the loss of the TE_{01} mode by almost 5 orders of magnitude, whereas the loss of the HE_{11} mode decreases by only a factor of 5.

In Fig. 3 the confinement loss at the least-loss wavelength of each mode is shown as a function of the number of rings for the modes in Fig. 2. The loss of all the modes shows an exponential dependence on the number of rings. It is clear from the difference in the slopes of the TE, HE, and TM modes that the TE-polarization guidance is much stronger; TM-polarization guidance is greatly suppressed. The HE modes have a TM-polarized component, and their confinement loss shows the same characteristics as the TM modes.⁹

The different modes have least-loss points at different wavelengths. The losses of the TE_{02} and HE_{11} modes at the least-loss wavelength of the TE_{01} mode are also shown in Fig. 3, as is the ratio of the loss of the second-lowest loss mode to the loss of the TE_{01} mode. This ratio is seen to increase exponentially, reaching approximately 70 for nine rings; i.e., the TE_{01} mode can propagate 70 times further than any other mode before suffering a given attenuation. This is the mechanism through which the TE_{01} mode is isolated, making the fiber effectively single mode with a polarization nondegenerate mode. In accordance with the research reported in Ref. 10, the length at which this design becomes effectively single mode, $L_{sm} = 0.7$ m, and the

maximum length over which it will usefully guide is $L_{max} = 24$ m. These values are only illustrative, and, as can be seen from Fig. 3, the loss of the TE_{01} mode can be decreased and the difference in the loss of that and the other modes increased by addition of more rings; this will increase L_{max} . Also, as discussed in Ref. 11, reducing the core size can greatly perturb the TE_{02} mode, increasing its loss to decrease L_{sm} .

We modeled the holey structure of the cladding by looking at the two-dimensional lattice of holes that forms asymptotically at increasing distance from the core (Fig. 4). To do this, we mapped the cylindrical geometry of the fiber to the Cartesian geometry of the resultant lattice by mapping the radial and azimuthal directions to the x and y directions, respectively, so

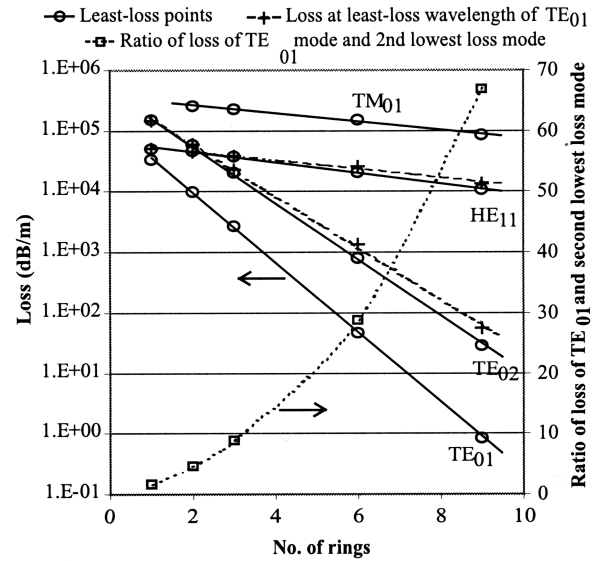


Fig. 3. Confinement loss of the least-loss wavelength as a function of the number of rings. For the HE_{11} and TE_{02} modes the loss at the least-loss wavelength of the TE_{01} mode is also shown. The ratio of the loss of the lowest-loss (TE_{01}) and the second-lowest-loss modes is also shown.

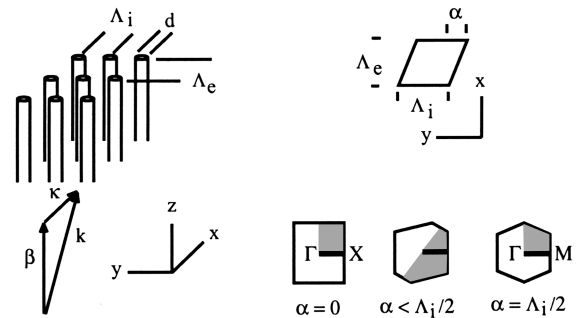


Fig. 4. Left, the two-dimensional lattice that forms asymptotically at increasing distance from the core with the wave vector restricted to the xz plane (κ and β are the x and z components, respectively). Right, unit cell and Brillouin zones with different y offsets α between adjacent layers in the x direction. The restricted wave vector means that only the path indicated (e.g., from Γ to X for $\alpha = 0$) needs to be considered, rather than the boundary of the irreducible Brillouin zone (shaded). Changes to the value of α were found to make negligible differences in the positions of the bands for the path considered.

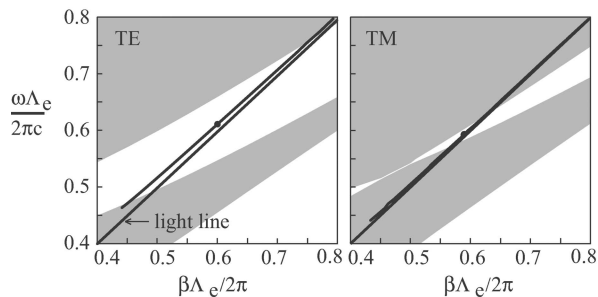


Fig. 5. Left, TE-polarization band diagram (gaps are indicated in white) with the position of the TE_{01} mode shown; the least-loss point is marked. Right, band diagram for TM polarization with the HE_{11} mode shown. The closing of the band near the light line suppresses the TM and HE modes.

that Λ_e and Λ_i correspond to the x and y pitches, respectively. For the TE- and TM-polarized modes in the fiber the wave vector is constrained to the rz plane, which maps to the xz plane.

The band diagram for the two-dimensional lattice was calculated using standard Fourier decomposition techniques¹² and is shown in Fig. 5. The placement of holes on rings concentric with the core and the restriction of the wave vector to the rz/xz plane means that only one direction in the irreducible Brillouin zone needs to be considered (the x direction). In general, the entire boundary of the irreducible Brillouin zone would need to be considered and a bandgap would need to remain open along all the directions on the boundary. In this case, the restrictions on direction mean that a partial gap is as good as a full gap. The partial gap is in the x direction and always occurs. The two-dimensional lattice is essentially reduced to behave as a one-dimensional multilayer stack.

The inclusion of conical incidence (the wave vector has a z component and so does not lie in the plane of periodicity) means that no strictly TE- or TM-polarized bands exist. However, it is clear which bands approximate TE and TM polarization from the dominant field components, as was the case for the fiber modes. In Fig. 5 a large TE bandgap can be seen, centered approximately on the least-loss wavelength, whereas the TM bandgap is seen to close near the light line, leaving

a much smaller gap, again centered on the least-loss wavelength. The point at which the TM band closes must be analogous to the Brewster angle phenomenon that would be observed if that lattice were replaced by a multilayer stack.¹¹ This point would be most effective if it were positioned to intersect the HE_{11} mode, meaning that the HE_{11} mode would always be outside the bandgap. We intend to carry out such optimization of the design in future research and to investigate fabrication of the design by using polymers, as described in Ref. 7.

The authors thank M. Large, R. McPhedran, and W. Padden for helpful discussions. The computer facilities at the Australian Partnership for Advanced Computing and Sydney Vislab were used for this study. A. Argyros's e-mail address is a.argyros@oftc.usyd.edu.au.

References

1. P. Russell, *Science* **299**, 358 (2003).
2. T. A. Birks, J. C. Knight, and P. St. J. Russell, *Opt. Lett.* **22**, 961 (1997).
3. R. F. Cregan, B. J. Managan, J. C. Knight, T. A. Birks, P. St. J. Russell, P. J. Roberts, and D. C. Allen, *Science* **285**, 1537 (1999).
4. J. Noda, K. Okamoto, and Y. Sasaki, *J. Lightwave Technol.* **4**, 1071 (1986).
5. A. Ferrando and J. J. Miret, *Appl. Phys. Lett.* **78**, 3184 (2001).
6. I. Bassett and A. Argyros, *Opt. Express* **10**, 1342 (2002), <http://www.opticsexpress.org>.
7. A. Argyros, I. Bassett, M. A. van Eijkelenborg, M. C. J. Large, J. Nagari, N. A. P. Nicorovici, R. C. McPhedran, and C. M. de Sterke, *Opt. Express* **9**, 813 (2001), <http://www.opticsexpress.org>.
8. N. Issa and L. Poladian, *J. Lightwave Technol.* **21**, 1005 (2003).
9. Y. Xu, A. Yariv, J. G. Fleming, and S.-Y. Lin, *Opt. Express* **11**, 1039 (2003), <http://www.opticsexpress.org>.
10. A. Argyros and I. Bassett, in *Proceedings of the Symposium on Optical Fibre Measurements (SOFM)* (U.S. GPO, Washington, D.C., 2002), p. 135.
11. A. Argyros, *Opt. Express* **10**, 1411 (2002), <http://www.opticsexpress.org>.
12. K. Sakoda, *Optical Properties of Photonic Crystals* (Springer-Verlag, Berlin, 2001).